A Coupled Thermal-Electromagnetic FEM Model to Characterize the Thermal Behavior of Power Transformers Damaged By Short Circuit Faults

Vahid Behjat

Department of Electrical Engineering, Engineering Faculty, Azarbaijan Shahid Madani University, Tabriz, Iran
Email: behjat@azaruniv.edu

Abstract—This research work is an initiative to characterize the thermal behavior of power transformers in presence of winding short circuit faults as one of the most important causes of failures in power transformers. The paper contributes for this matter by accurately estimating the excessive power losses and temperature rise due to winding short circuit faults, through a circuit-magnetic-thermal FEM coupling method. The magnetic-circuit coupled FEM model of the faulty transformer allows the computation of the circulating current in the shorted turns, flux distribution in the transformer and the power dissipated by Joule effect in the shorted region of the winding. Once the local losses, required as heat sources for the thermal analysis, are calculated, a coupled electromagnetic-thermal FEM model of the transformer is developed to solve the transient heat flow equations and obtain the transient thermal characterization of the transformer damaged by short circuit faults. At each time step in the coupled transient FEM thermal model, a local linking of thermal and then steady state AC magnetic computations is carried out, as a means of better representation of the transformer dynamic thermal behavior.

Index Terms—power transformer, thermal performance, finite element method, winding short circuit fault, coupled transient thermal model

I. INTRODUCTION

A study of the records of the modern transformer breakdowns, which occurred over a period of years, showed that nearly seventy percent of the total number of the power transformer failures are eventually traced to undetected short circuit faults [1] and [2]. Therefore, it is essential to detect and localize the fault at an early stage so that preparations for necessary corrective action can be planned in advanced and executed quickly [3]. To make an accurate fault detection system, analyzing the local and global effects of the fault on the transformer behavior is inevitable.

Traditionally, thermal studies of transformers have been carried out by analytical techniques [4]-[9], or by different kinds of equivalent thermal circuits [10]-[12]. A literature review indicates that there are some research efforts dealing with thermal FEM models of transformers which are mainly focused on prediction of the windings and the core hot spot temperature and location [4]-[14]. In addition, various implementations of the finite element thermal models for investigating the thermal performance of the transformers subjected to harmonic currents [15]-[17] and nonlinear loads [18]-[19], as well as transformers with particular structures of the windings [20], high frequency [21] and planar transformers [22] have been reported. However, in spite of extensive literature survey on different aspects of the transformer thermal modeling, prediction and characterization of the transformer thermal behavior in the presence of short circuit faults, also quantifying the increased winding losses due to the short circuit faults and the corresponding temperature rise in the transformers are the issues, so far, remain unreported and therefore form the subject matter of this paper. This is accomplished using a 2-D coupled electromagnetic-thermal FEM model adapted for introducing a power transformer with internal winding short circuit faults. Coupling of electromagnetic and thermal FEM analysis is also employed in the developed FEM model, as a means of better representation of the transformer dynamic thermal behavior. There are several approaches for coupled transient computation of the interacting electromagnetic-thermal fields in electrical machines containing significantly different time constants, which are discussed in reference [23]-[27]. In fact, the main contribution of the present paper is to extend the methods of [23]-[27] to include the short circuit faults in the transformers thermal model as well as characterizing the transformer thermal behavior in this condition.

The paper is organized as follows. Section II presents a brief description addressing the characteristics of the considered transformer and also outlines the principles of the magnetic field modeling of the transformer damaged by short circuit fault. The third section focuses on thermal field modeling of the faulty transformer. In Section IV the algorithm used for solving the coupled electromagnetic-thermal problem is described. The practical application and the detailed discussions on the results, also implications for future researches are illustrated in Section V. Finally conclusions will be given in the last section.

II. MAGNETIC FIELD MODELING OF A TRANSFORMER WITH WINDING SHORT CIRCUIT FAULT

A. Characteristics of the Considered Transformer

The FEM simulations are carried out on a three phase, two winding, 50Hz, 100kVA, 35kV/400V, Yzn5, oil immersed, ONAN, core type distribution transformer. The transformer is employed in simulations with all the parameters and configuration provided by the manufacturer. The LV winding consists of 2 layers, each layer comprising 30 turns of copper wire (4×10.5mm2cross-sectional area), and is wound around each leg of core separated by one layer of insulation. Each HV winding contains 16 discs of 336 stranded copper wire (round type enameled copper wire 1mm diameter), and is separated by one layer of insulation from the LV winding.

B. Circuit-Magnetic Coupled FEM Formulation

The governing equation of the time dependent electromagnetic model in 2-D Cartesian coordinates based on the A-V-A formulation is derived from the Maxwell's equations using the magnetic vector potential, A[Wb/m], and electric scalar potential, V[v], [28].

$$\nabla \times (\nu_0 [\nu_r] \nabla \times A) + [\sigma](\frac{\partial A}{\partial t}) + \nabla V) = 0 \quad (1)$$

where $[\nu_r]$ is the tensor of the reluctivity of the medium, $[\nu_0]$ is the reluctivity of the vacuum (in m/H), A is the magnetic vector complex potential (in Wb/m), $[\sigma]$ is the tensor of the conductivity of the medium (in S) and V is the electric scalar potential (in V). To simulate the behavior of the transformer in presence of winding short circuit faults, coupling between electric circuit and magnetic fields is required. Generally the electric circuit branch equations can be written in the following matrix form [29]:

$$[e_m] = [R_m][i_m] + \frac{d}{dt}[\Phi_m] + [L_m]\frac{d}{dt}[i_m] \quad (2)$$

In this matricidal expression, for a branch m, Φ_m represents the magnetic circuit flux linkage, e_m and i_m are the voltage drop and the current respectively, R_m and L_m are the resistance and the leakage inductance respectively. Each of the electromagnetic and the electric circuit fields yields its own matrix equations, which are directly coupled and solved simultaneously. To obtain a unique solution for the governing equations based on the A-V-A formulation, the divergence of the vector potential, A, is specified using the Coulomb gauge ($\nabla \cdot A = 0$) and the zero Dirichlet boundary condition is applied on the external border of the computation domain.

The principle used in this study for modeling short circuit faults on the transformer windings is to divide the winding across which the fault occurs in two parts: the short-circuited part and the remaining coils in the circuit [30]. It should be pointed out that when a short circuit fault occurs on the transformer windings, the picture of the electromagnetic field inside the transformer will be altered totally as well as the current in the circuit domain

[31]. However, the electromagnetic behavior of the faulty transformer still satisfies the Maxwell equations. This means that solving the electromagnetic field in a faulty transformer is reduced again to solving the mentioned coupled field-circuit governing equations (1-3). Therefore with the developed circuit coupled FEM model of the transformer, a whole variety of short circuit faults can be simulated with different levels of severity and size and at different locations along the windings.

C. 2D Electromagnetic FEM Model

In general, the magnetic field modeling of the transformer can be distinguished into three parts: the core, the windings and the oil surrounding the active part of the transformer. In the developed FEM model for the considered transformer, the core and the surrounding oil were entirely included in the model. The nonlinear magnetization characteristics of the iron was input manually into the solver and assigned to the transformer core. Regarding the windings, their representation is related to the modeling of the skin effect. The skin depth (δ) of a medium is defined by the following expression:

$$\delta = \sqrt{\frac{2}{\sigma \omega \mu_0 \mu_r}} \quad (3)$$

where ω is the supply frequency, μ_0 the vacuum permeability, μ_r the relative permeability and σ is the conductivity of the medium. The thickness of the skin depth area of the winding conductors at 50 Hz based on the values $\mu_r=1$ and $\sigma=59.6e6$ S/m of the copper properties is about 9.2 mm, which joule losses are concentrated on this thin layer. Thus, HV windings of the considered transformer, having a value of the skin depth much greater than the dimensions of the conductor's cross section, are characterized by an almost uniform distribution of the current density over all the conductor cross section and as a consequence modeled by stranded coil conductors. However, LV windings with conductors having dimensions of cross section comparable to the value of the skin depth were modeled by solid conductors. Finally, by coupling all the regions in the finite element domain to the circuit domain, the 2D FEM model was completed.

III. THERMAL FIELD MODELING

The basic relations of conduction heat transfer which describe transient temperature distribution in the solution region are the Fourier's law and the equation of heat conduction [32]:

$$\varphi = -[k]\nabla T \quad (4)$$

$$\nabla \cdot \varphi + \rho C_p \frac{\partial T}{\partial t} = q \quad (5)$$

where φ is the heat flux density (in W/m^2), [k] is the tensor of thermal conductivity (in W/m/K), ρC_p is the volumetric heat capacity (in J/m^3/K) and q is the volume density of power of the heat sources (in W/m^2). The equation to be solved in a transient thermal application is the following [33]:

$$\nabla.(-k\nabla T) + \rho C_p \frac{\partial T}{\partial t} = q \qquad (6)$$

The above equations describe heat transfer by thermal conduction within the solid bodies of the temperature computation domain. The conditions of uniqueness of the solution of the heat transfer equation are the initial conditions and the boundary conditions at the surface of the solid bodies. The initial condition specifies the temperature distribution at time zero:

$$T(x,y,0) = T_0(x,y) \qquad (7)$$

We will set the ambient temperature to 30 ℃ and use as initial temperature map of the study domain. Thermal convection heat transfer characterizes the boundaries of solid regions of the studied device and the surrounding fluid as below:

$$\varphi.n = -h(T - T_a) \qquad (8)$$

where h is the convection heat exchange coefficient in (W/m^2/K), Ta is the ambient temperature in Kelvin and n is the unit outward normal to the surface of the solution domain. In general, the value of the heat transfer coefficient h is a complicated function of the fluid flow, the thermal properties of the fluid medium and the geometry of the system. Such a broad dependence makes it difficult to obtain an analytical expression for the heat transfer coefficient. In the heat transfer literature, it is customary to represent the h value by the dimensionless Nusselt number Nu [33].

$$Nu = \frac{h.L}{k} \qquad (9)$$

where L is the dimension of the flow passage and k is the thermal conductivity. Typically, the Nusselt number is expressed as a function of two other dimensionless numbers, namely, the Grashof number (Gr) and the Prandtl number (Pr) [33]:

$$Nu = C(Gr.\mathrm{Pr})^n \qquad (10)$$

where C and n are empirical constants dependent on the oil circulation. The Grashof and Prandtl number are calculated by (11) and (12) respectively [33]:

$$\mathrm{Pr} = \frac{C_p \mu}{k} \qquad (11)$$

$$Gr = \frac{g\beta\Delta\theta L^3 \rho^2}{\mu^2} \qquad (12)$$

where g is the gravitational constant (m/s^2), β is the thermal expansion coefficient of the oil (1/℃), L is the characteristic dimension (m), ρ is the oil density (kg/m^3), K is the oil thermal conductivity (w/m/℃), Cp is the specific heat of the oil (J/kg/°C), μ is the oil viscosity (kg/ms) and Δθ is the top-oil to ambient temperature gradient (℃). It is generally valid for all transformer insulation oils that the variation of the oil viscosity with temperature is much higher than the variation of the other oil parameters. Thus, all oil physical parameters except the viscosity in (13) can be replaced by a constant.

$$\mu = A_1 e^{(\frac{A_2}{\theta_{oil}+273})} \qquad (13)$$

The thermal field modeling of the considered transformer starts with calculation of all the constants in the equations (4)–(13) based on the material properties of the selected transformer, analytical formulas extracted from heat transfer theories, and the empirical coefficients provided by the manufacturer. Afterwards, the model is completed by assigning thermal specifications of the materials to the solid and the fluid components of the transformer and then assigning the value of the heat transfer coefficient h to the boundaries of the solid regions and the surrounding oil. The computation domain in the thermal field model of the considered transformer includes all the solid parts of the transformer, i.e. the core, the LV and HV windings, the insulations and the fluid component i.e. the surrounding oil. In the developed FEM model of the transformer, the windings and the core are defined from the magnetic and thermal points of view and the thermal exchanges surface on the boundaries of the study domain is defined only from the thermal point of view.

To address the composition of insulations and conductors in the transformer windings, the HV windings are represented by a single isotropic thermal conductivity because of dense stranded conductors in its structure and symmetry of the conductor and insulation materials, calculated using a weighted average, based on the volume fractions as follows [17]:

$$K_{eq} = \frac{K_{cond}V_{cond} + K_{insul}V_{insul}}{V_{cond} + V_{insul}} \qquad (14)$$

Similar formulae developed to be used for the ρ and the C parameters. For the case of the LV windings, since theirs conductors are solid type, so they are better represented by an anisotropic thermal conductivity. The thermal conductivities along and across the layers of the LV winding depends not only on the thermal conductivities of the copper, Kcond, and the insulation material, Kinsul, but also on the relative thickness of each along the paths of the heat travel. Thus, for the LV winding, the equivalent thermal conductivity in the tangential direction, where the conductor and the insulation layers are in parallel and in the radial direction (perpendicular to winding layers), where the conductor and the insulation layers are in series, are calculated by the following equations:

$$K_t = \frac{K_{cond}d_{cond} + K_{insul}d_{insul}}{d_{cond} + d_{insul}} \qquad (15)$$

$$K_r = \frac{1/(\frac{1}{K_{cond}d_{cond}} + \frac{1}{k_{insul}d_{insul}})}{d_{cond} + d_{insul}} \qquad (16)$$

In the above equations, the equivalent tangential and radial thermal conductivity of the winding are denoted by the indices t and r, respectively. In addition, d_{cond} and d_{insul} are the thickness of the copper and the insulation of the LV winding, respectively. Based on the above

explanations and equations, the values for thermal specifications are calculated and assigned to the LV and HV windings of the considered transformer. By applying the specifications of the other components of the transformer and the boundary conditions to the thermal exchanges surfaces, the model will be ready for the solving process based on the developed computation algorithm, which will be explained in detail in the following section.

IV. MAGNETO-THERMAL COUPLED PROBLEM COMPUTATION

The magneto thermal coupling proposed in this study is a coupling between the steady state AC magnetic computation, which allows the estimation of the active power loss dissipated by the Joule effect in the heated components of the considered transformer, and the transient thermal computation, which allows the study of the temperature evolution in the heated components of the transformer.

It is worth pointing out that in spite of the field-circuit coupling in Section III, in the developed magneto-thermal coupling method, due to large differences in the time constants of the magnetic and thermal fields, two systems of the equations (Maxwell's and Fourier's equations) are separately and not simultaneously solved. Indeed, from the thermal point of view, the value of the time constant of a transient thermal phenomenon is much higher than the electromagnetic time constant. However, to treat a simultaneously solving of equations, there is only one "time step" variable for all the phenomena involved in the coupling problem. Needless to emphasize an exact transient solution requires that the related time-step is at least smaller than the smallest time constant of the problem, but it is obvious that adapting the time step of the magnetic-thermal coupling problem to the smaller time constant (magnetic), will lead to prohibitive computation times. To overcome this difficulty and reaching acceptable values of the computation times, the magneto-thermal coupling method used in this is based on separately and successively solving of the magnetic field and the transient thermal equations for each time step and then transferring the results between the two sets of the equations.

Result transferring means that the power losses obtaining from the magnetic computation, is introduced as heat sources of the system of the thermal equations. On the other side, the temperature resulting from the thermal computation is considered for evaluation of the material characteristics in the magnetic equations to meet the temperature dependence of the electromagnetic properties like as magnetic permeability, electric resistance and permittivity. The principle of the magneto thermal coupling is detailed in Fig. 1.

At each time step, a local linking of thermal and magnetic computations is carried out, until the steadiness of the temperature field corresponding to the analyzed time step is achieved. To control the iterative process of the thermal updating, a stopping criterion which defines the precision of the updating process is defined. Another

stopping criterion is defined to control the maximum number of the iterations; this criterion sets the maximal number of the iterations and allows stopping of the solving process in case of non-convergence of the thermal updating process.
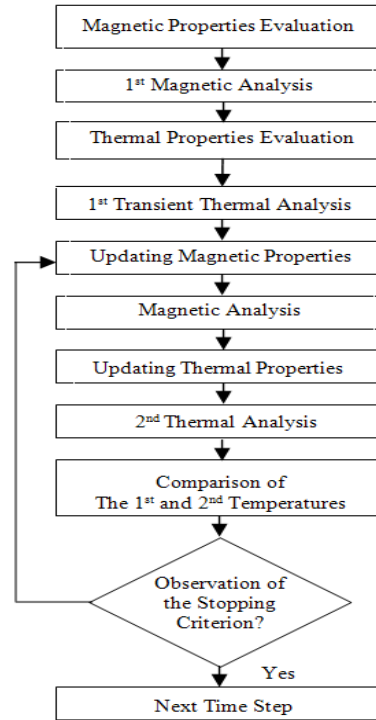
Figure 1. Magneto-thermal coupled problem computation flow chart.

V. RESULTS & DISCUSSION
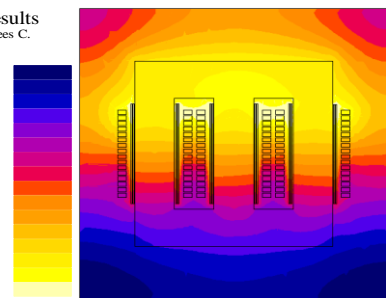
Figure 2. Color shaded plot of the temperature distribution inside the transformer at 0.9 rated load.
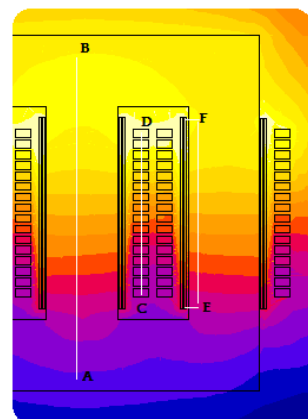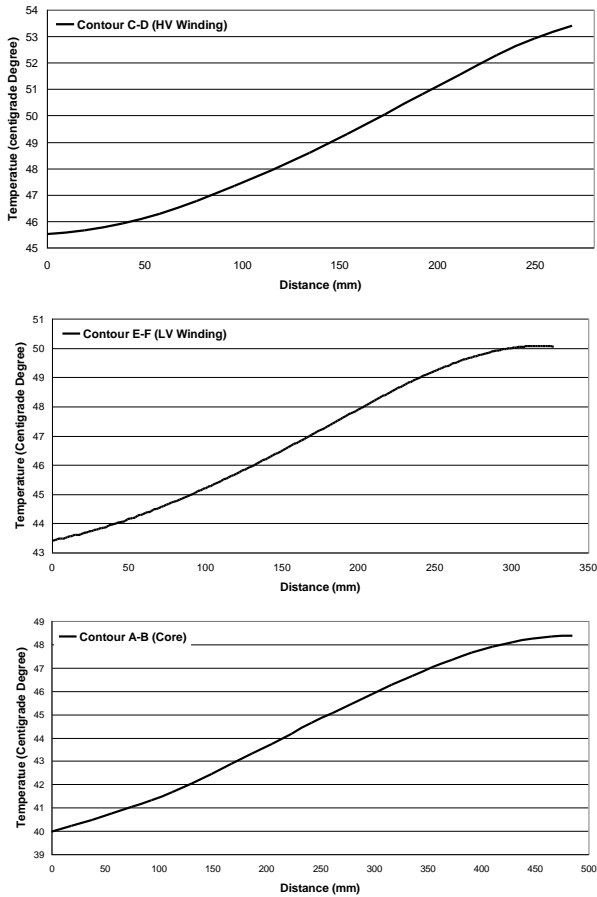
Figure 3. Temperature variation along the contours on the transformer surface, normal and full-load operating condition of the transformer.

After applying the inputs and the boundary conditions described in the previous sections, the coupled FEM model was solved for prediction of the thermal performance in the selected transformer, operating under healthy and different short circuit fault conditions. The space distribution of the temperature inside the transformer, operating under healthy condition, 0.9 nominal load and constant ambient temperature of 30 ℃ is illustrated in Fig. 2. A zoomed color shaded plot of the temperature distribution at rated load with the plots of the temperature variation along the contours on the transformer surface is given in Fig. 3. As it can be readily seen from the simulation results in the Fig. 2 and Fig. 3, the temperature is increased from the bottom to the top inside the transformer and the hot spot of the windings is always placed on the top part of the transformer. However, the temperature of the hot spot of the LV and HV windings differs due to the windings type and thickness of the their insulation layer.

Fig. 4 shows the temperature density plot and isothermal lines of the transformer working at rated load and for a short circuit fault along the second turn of the LV winding from the neutral point. The color shaded plot of the temperature distribution inside the transformer when a short circuit fault is imposed on the turns of the outermost layer of the second disc from the line end of the HV winding is depicted in Fig. 5. Considering Figs.

4-5 and comparing them with Fig. 2, clearly reveals that the introduced short circuit fault on the windings yields higher hot spot temperatures and the hot spot point is transferred from top of the windings at the healthy condition to the shorted region at fault conditions.
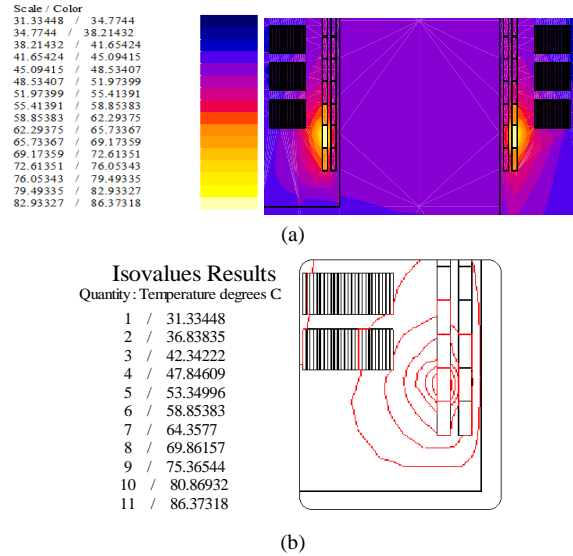
Figure 4. Temperature distribution inside the considered transformer after arising the short circuit fault along the 2nd turn from the line end of the LV winding on phase "U", (a) Temperature density plot, (b) Isothermal lines.
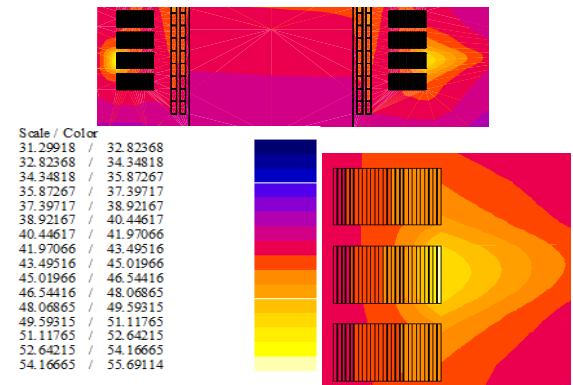
Figure 5. Color shaded plot of the temperature density inside the selected transformer damaged by a short circuit fault between the turns of the outermost layer of the 2nd HV disk from the neutral point on phase "U".

TABLE I. CORRESPONDING VALUES OF THE HV WINDING HOT SPOT TEMPERATURE AND THE TRANSFORMER DIFFERENTIAL CURRENT IN NORMAL OPERATING CONDITION AND FOR INTERTURN FAULTS INVOLVING 0.2% OF THE TURNS ON HV WINDING OF THE TRANSFORMER WITH THREE LEVELS OF SEVERITY (RFH1>RFH2>RFH3)

Fault Case	Idiff (%rated current)	Hotspot Temp (∘C)
Normal Condition	0.00%	53.13
RFH1	0.05%	55.70
RFH2	0.28%	64.71
RFH3	0.80%	86.88

To better characterize the thermal performance of the transformer damaged by short circuit faults, additional simulations were performed with different degree of fault severity in the shorted turns. Table I, illustrates the HV

winding hot spot temperature as well as the transformer differential current in presence of faults with three different resistance values, denoted by FH1 to FH3 indexes for the faults occurring between 0.2% of the turns on phase "U" of the HV winding. In all of the considered fault scenarios, the load and supplying voltage of the transformer is kept constant at their nominal values. Observing the given results in Table I, it becomes evident that when the transformer is in normal condition, the turn dielectric is almost perfect, the terminal current and the winding average and hot spot temperatures are very close to the rated values and the differential current is nearly zero. However, during the exercise of decreasing the value of the fault resistance, i.e. increasing the fault severity level, a significant increasing trend is visible in the relative change of the winding hot spot temperature, while the transformer differential current is increasing much more slowly.

Inordinate temperature rise due to the short circuit fault occurrence along the winding is mainly due to DC heat losses in the copper windings, which vary with the square of the rms circulating current. Thus, the increasing trend of the winding hot spot temperatures is a result of great circulating current in the shorted turns which in turn is a result of high ratio of transformation between the whole winding and the shorted turns. In fact, for a short circuit fault involving a low fraction of the winding, the circulating current in the shorted turns increases more significantly than the terminal current. This would seem to present a problem for fault detection at its incipient stage where it would be very difficult to detect a change in the terminal current caused by the fault in spite of the drastic circulating current and severe localized heating in the shorted turns. It should be remarked that all the considered fault cases in Table I, cannot be detected with the overall sensitivity represented by the over-current or restrained differential protections, as the base protections of the power transformers against internal faults, with a sensitivity of 20%-30% rated current.

With all the above observations, one can conclude that early stages of winding short circuit faults have negligible effects on the transformer terminal performance. However, additional power loss and localized thermal overloading in the shorted region, sustains favorable conditions for the fault to accelerate the insulation degradation and rapidly spread to a larger section of the winding, which would result in more serious permanent faults and irreversible damage to the transformer. Accordingly, significant advantages would accrue by development of online, reliable and sensitive short circuit fault detection methods, which constitutes one of the future directions of this research.

VI. Conclusion

It was demonstrated in this study, for the first time, how winding short circuit faults affect the thermal behavior of a real transformer. Space distribution and transient evolution of the temperature in the heated components of the damaged transformer was accomplished using a 2D transient coupled electromagnetic-thermal FEM model. From the simulations made on the considered transformer, it can be concluded, during a short circuit fault on the transformer winding, the circulating current in the shorted turns causes additional power loss, severe localized heating and abnormal temperature rise in the shorted region. However, the transformer terminal modification is too small to identify cleanly and the fault left undetected until it evolves into a high level fault with more severe damage to the transformer. Characteristic signatures associated with short circuit faults extracted from the transformer thermal behavior are expected to yield insights in developing reliable and sensitive fault detection and localization methods in power transformers.

References

[1] W. Bartley, "Analysis of transformer failures," in *Proc. International Association of Engineering Insurers 36th Annual Conference*, Stockholm, Sweden, 2003.

[2] S. A. Stigant and A. C. Franlin, The J and P Transformer Book: A Practical Technology of the Power Transformer, 10th ed., New York: Wiley, 1973.

[3] V. Behjat, A. Vahedi, A. Setayeshmehr, H. Borsi, and E. Gockenbach, "Identification of the most sensitive frequency response measurement technique for diagnosis of interturn faults in power transformers," *IOP Publishing (Measurement Science and Technology), Meas. Sci. Technol. 21 (2010) 075106 (14pp)*, pp. 1-14, 2010.

[4] A. Rele and S. Palmer, "Determination of temperature in transformer winding," *IEEE Trans.*, PAS-94, vol. 5, pp. 1763–1769, 1975.

[5] J. E. Lindsay, "Temperature rise of an oil-filled transformer with varying load," *IEEE Trans.*, PAS-103, vol. 9, pp. 2530–2535, 1984.

[6] IEEE Guide for Loading Mineral-Oil-Immersed Transformers, IEEE Standard C57.91-1995 (R2002), Jun. 2002.

[7] L. Pierce, "An investigation of the temperature distribution in cast-resin transformer windings," *IEEE Trans. Power Delivery*, vol. 7, no. 2, pp. 920–926, Apr. 1992.

[8] L. Pierce, "An investigation of the thermal performance of an oil filled transformer," *IEEE Trans. Power Delivery*, vol. 7, no. 3, pp. 1347–1358, July 1992.

[9] M. K. Pradhan and T. S. Ramu, "Prediction of hottest spot temperature (HST) in power and station transformers," *IEEE Trans. Power Delivery*, vol. 18, pp. 1275–1283, Oct. 2003.

[10] G. Swift, T. Molinski, and W. Lehn, "A fundamental approach to transformer thermal modeling—Part I: Theory and equivalent circuit," *IEEE Trans. Power Delivery*, vol. 16, no. 2, pp. 171–175, Apr. 2001.

[11] D. Susa, M. Lehtonen, and H. Nordman, "Dynamic thermal modeling of power transformers," *IEEE Trans. Power Delivery*, vol. 20, no. 1, pp. 197–204, Jan. 2005.

[12] A. Elmoudi, M. Lehtonen, and Hasse Nordman, "Thermal model for power transformers dynamic loading," in *Proc. Conference Record of the 2006 IEEE International Symposium on Electrical Insulation*, 2006, pp. 214-217.

[13] J. Faiz, M. B. B. Sharifian, and A. Fakhri, "Two-dimensional finite element thermal modeling of an oil-immersed transformer," *Euro. Trans. Electr. Power*, vol. 18, no. 6, pp. 577–594, Sep. 2007.

[14] E. G. teNyenhuis, R. S. Girgis, G. F. Mechler, and G. Zhou, "Calculation of core hot-spot temperature in power and distribution transformers," *IEEE Trans. Power Delivery*, vol. 17, no. 4, pp. 991–995, Oct. 2002.

[15] M. D. Hwang, W. M. Grady, and H. W. Sanders, "Calculation of winding temperatures in distribution transformers subjected to harmonic currents," *IEEE Trans. Power Delivery*, vol. 3, no. 3, pp. 1074–1079, July 1988.

[16] J. Driesen, T. Van Craenenbroeck, B. Brouwers, K. Hameyer, and R. Belmans, "Practical method to determine additional load losses due to harmonic currents in transformers with wire and foil

windings," *in Proc. Power Eng. Soc. Winter Meet.*, vol. 3, 2000, pp. 2306–2311.

[17] J. Driesen, K. Hameyer, and R. Belmans, "The computation of the effects of harmonic currents on transformers using a coupled electromagnetic-thermal FEM approach," *in Proc. 9th Int. Conf. Harmonics Quality Power*, vol. 2, Oct. 2000, pp. 720–725.

[18] A. Lefevre, L. Miegeville, J. Fouladgar, and G. Olivier, "3D-Computation of transformers overheating under nonlinear loads," *IEEE Trans. Magn.*, vol. 41, no. 5, pp. 1564–1567, May 2005.

[19] M. I. Samesima, J. W. Resende, and S. C. N. At-aujo, "Analysis of transformer loss of life driving nonlinear industrial loads by the finite elements approach", *IEEE,* 1995, pp. 2175-2179.

[20] M. K. Pradhan and T. S. Ramu, "Estimation of the Hottest Spot Temperature (HST) in power transformers considering thermal inhomogeniety of the windings," *IEEE Trans. Power Delivery*, vol. 19, no. 4, pp. 1704-1712, Oct. 2004.

[21] C. C. Hwang, P. H. Tang, and Y. H. Jiang, "Thermal analysis of high frequency transformers using finite elements coupled with temperature rise method," *IEE Proc. Elect. Power Appl.*, vol. 152, no. 4, pp. 832–836, Jul. 2005.

[22] C. Buccella, C. Cecati, and F. D. Monte, "A coupled electrothermal model for planar transformer temperature distribution computation," *IEEE Trans. Industrial Electronics*, vol. 55, no. 10, pp. 3583-3590, Oct. 2008.

[23] J. Driesen, K. Hameyer, and R. Belmans, "The computation of the effects of harmonic currents on transformers using a coupled electromagnetic-thermal FEM approach", *in Proc. 9th Int. Conf. Harmonics Quality Power*, vol. 2, Oct. 2000, pp. 720–725.

[24] M. A. Tsili, E. I. Amoiralis, A. G. Kladas, and A. T. Souflaris, "Hybrid numerical-analytical technique for power transformer thermal modeling", *IEEE Trans Magnetics*, vol. 45, no. 3, pp. 1408-1411, March 2009.

[25] K. Preis, O. Biro, G. Buchgraber, and I. Ticar, "Thermal-electromagnetic coupling in the finite-element simulation of power transformers," *IEEE Trans. Magn.*, vol. 42, no. 4, pp. 999–1002, Apr. 2006.

[26] M. A. Tsili, A. G. Kladas, P. S. Georgilakis, A. T. Souflaris, and D. G. Paparigas, "Advanced design methodology for single and dual voltage wound core power transformers based on a particular finite element model," *Elect. Power Syst. Res.,* vol. 76, pp. 729–741, 2006.

[27] J. Driesen, R. J. M. Belmans, and K. Hameyer, "Methodologies for coupled transient electromagnetic-thermal finite-element modeling of electrical energy transducers," *IEEE Trans. Industry App.*, vol. 38, no. 5, pp. 1244-1250, Sep./Oct. 2002.

[28] B. Guru and H. Hiziroğlu, *Electromagnetic Field Theory Fundamentals,* Cambridge, U.K: Cambridge University Press, 2nd ed. 2004.

[29] F. Piriou and A. Razek, "Numerical simulation of a non-conventional alternator connected to a rectifier," *IEEE Tran. Energy Conversion*, vol. 5, no. 3, pp. 512-518, Sep. 1990

[30] A. Vahedi and V. Behjat, "Online monitoring of power transformers for detection of internal winding short circuit faults using negative sequence analysis," *European Trans. on Electrical Power*, vol. 21, pp. 196–211, 2011.

[31] V. Behjat and A. Vahedi, "A DWT based approach for detection of interturn faults in power transformers," *COMPEL: The International Journal for Computation and Mathematics in Electrical and Electronic*, vol. 30, no. 2, pp. 483-504, 2011.

[32] F. P. Incropera and D. P. DeWitt, *Fundamentals of Heat and Mass Transfer*, Hoboken, N. J.: John Wiley & Sons, Inc., 5th ed. 2002.

[33] M. N. Ozisik, Heat Transfer—A Basic Approach, *McGraw-Hill*: New York, 1985.

Vahid Behjat was born in 1980 in Tabriz, Iran. He received the B.Sc. degree in electrical engineering from the University of Tabriz, Tabriz, Iran, in 2002, and the M.Sc. and Ph.D. degrees in electrical engineering from Iran University of Science & Technology (IUST), Tehran, Iran, in 2002 and 2010, respectively.Currently, he is an Assistant Professor in the Department of Electrical Engineering, Azarbaijan Shahid Madani University, Tabriz. His main research interests include diagnostics and condition monitoring of power transformers and electrical machines, and the application of finite element method to design, modeling, and optimization of electrical machines.